



Published in final edited form as:

Eur Radiol. 2015 July ; 25(7): 1993–2003. doi:10.1007/s00330-015-3595-5.

Early survival prediction after intra-arterial therapies: a 3D quantitative MRI assessment of tumour response after TACE or radioembolization of colorectal cancer metastases to the liver

Julius Chapiro, MD^{1,2}, Rafael Duran, MD¹, MingDe Lin, PhD^{1,3}, Rüdiger Scherthaner, MD¹, David Lesage, PhD⁴, Zhijun Wang, MD, PhD¹, Lynn Jeanette Savic^{1,2}, and Jean-François Geschwind, MD¹

¹ Russell H. Morgan Department of Radiology and Radiological Science, Division of Vascular and Interventional Radiology, The Johns Hopkins Hospital, Sheikh Zayed Tower, Ste 7203, 1800 Orleans St, Baltimore, MD, USA 21287

² Department of Diagnostic and Interventional Radiology, Charité Universitätsmedizin Berlin, Germany

³ U/S Imaging and Interventions (UII), Philips Research North America, Briarcliff Manor, NY, USA

⁴ Philips Research, Medisys, Suresnes, France

Abstract

Objectives—This study evaluated the predictive role of 1D, 2D and 3D quantitative, enhancement-based MRI regarding overall survival (OS) in patients with colorectal liver metastases (CLM) following intra-arterial therapies (IAT).

Methods—This retrospective analysis included 29 patients who underwent transarterial chemoembolization (TACE) or radioembolization and received MRI within 6 weeks after therapy. Tumour response was assessed using 1D and 2D criteria (such as European Association for the Study of the Liver guidelines [EASL] and modified Response Evaluation Criteria in Solid Tumors [mRECIST]). In addition, a segmentation-based 3D quantification of overall (volumetric [v] RECIST) and enhancing lesion volume (quantitative [q] EASL) was performed on portal venous phase MRI. Accordingly, patients were classified as responders (R) and non-responders (NR). Survival was evaluated using Kaplan–Meier analysis and compared using Cox proportional hazard ratios (HR).

Results—Only enhancement-based criteria identified patients as responders. EASL and mRECIST did not predict patient survival ($P = 0.27$ and $P = 0.44$, respectively). Using uni- and multivariate analysis, qEASL was identified as the sole predictor of patient survival (9.9 months for R, 6.9 months for NR; $P = 0.038$; HR 0.4).

Conclusion—The ability of qEASL to predict survival early after IAT provides evidence for potential advantages of 3D quantitative tumour analysis.

Keywords

Liver cancer; Colorectal cancer; Metastases; Magnetic resonance imaging; Chemoembolization

Introduction

Colorectal cancer is the third most common neoplasm and the second leading cause of cancer-related death worldwide [1]. Metastatic colorectal cancer (mCRC) is diagnosed in up to 65 % of all colorectal cancer patients with the liver as the most common metastatic site [2]. Of those patients, only a minority are eligible for liver tumour resection with curative intent [3]. Within the last decade, the introduction of more effective chemotherapeutic agents showed some survival benefits in non-resectable patients with liver-dominant disease [4]. However, finding the right balance between efficacy and toxicity of systemic chemotherapy is particularly challenging in patients with late-stage mCRC. The occurrence of chemoresistance provides the opportunity for intra-arterial therapies (IAT) to fill the gap by delivering high doses of cytotoxic agents or internal radiation directly to the tumour while reducing systemic toxicity [5]. Thus, several loco-regional IATs such as hepatic arterial infusion, transarterial chemoembolization (TACE) and yttrium-90 (Y90) radioembolization have been investigated and showed encouraging data regarding safety, toxicity and patient survival [6–9].

While overall survival (OS) continues to be the ultimate end point of clinical cancer research, most trials rely on imaging biomarkers in order to assess local tumour status as well as to compare the efficacy of different intra-arterial modalities [10, 11]. The primary clinical purpose of follow-up imaging, however, remains to reliably identify non-responders early after the treatment with the goal of improving therapeutic decisions. The majority of available protocols use the unidimensional (1D) Response Evaluation Criteria in Solid Tumors (RECIST) for the assessment of tumour response in mCRC. However, more recent literature suggests the use of modified RECIST (mRECIST) as well as the bidimensional (2D) European Association for the Study of the Liver (EASL) guidelines to assess tumour response after IAT on contrast-enhanced MRI (ceMRI) [12–16]. Most IATs involve an element of embolization of tumour-feeding arteries, thus causing tissue necrosis without immediate effects on the overall lesions size. This mechanism limits the value of anatomic, non-functional measurements such as RECIST [17–20]. Additionally, there are considerable limitations of all 1D and 2D assessment techniques including their limited reproducibility as well as their inability to evaluate the entire lesion, making them anatomically inaccurate in predicting the true extent of the mostly heterogeneous tumour necrosis [15, 21, 22]. This has been recognized by a multidisciplinary research consensus panel on mCRC management, and their recommendation to address this limitation is to develop new imaging-based tumour response criteria. The panel concluded with this as a high priority research topic [19]. The introduction of three-dimensional (3D) quantitative MRI techniques for the assessment of liver tumours may prove to be promising alternatives [22–25]. However, little is known about the role of these techniques in the assessment of tumour response of mCRC after IAT.

This study evaluated the predictive role of 1D, 2D and 3D quantitative, enhancement-based MRI assessment techniques as predictive markers for patient survival early after IATs in patients with mCRC to the liver. Specifically, this study compared the predictive value of the non-3D techniques (RECIST, WHO, EASL, mRECIST) with the new methods, to which we will herein refer to as volumetric RECIST (vRECIST) and quantitative EASL (qEASL).

Methods

Study cohort

This single-institution study was conducted in compliance with the Health Insurance Portability and Accountability Act and approved by the institutional review board. Between December 2005 and December 2012, a total of 49 patients with liver-only or liver-dominant mCRC underwent their first session of IAT within our institution. Treatment options for all patients were discussed at a multidisciplinary liver tumour board and the decisions regarding treatment modality were made on a case-by-case basis, as described elsewhere [8]. All patients included in the study had disease progression after systemic chemotherapy. Figure 1 illustrates the process of patient selection. Patients who received additional liver-directed therapies such as external-beam radiation or radiofrequency ablation of the index lesions prior to the first session of IAT were excluded from the analysis ($N = 10$). All included patients had received dynamic contrast-enhanced MRI within 6 weeks before and after the initial IAT session (excluding $N = 9$). Additionally, one patient was excluded because of an unclear histopathological classification of the dominant liver lesion. The remaining 29 patients, treated with conventional TACE (cTACE) or Y90 radioembolization, were included into the final analysis.

Evaluation and staging

All included patients underwent a full clinical examination as well as baseline laboratory tests (liver function; serum albumin, prothrombin time, total bilirubin, aspartate transaminase, alanine transaminase). Eastern Cooperative Oncology Group (ECOG) performance status was recorded in all patients.

Intra-arterial therapy

All procedures were performed by one experienced interventional radiologist (J.F.G. with 16 years of experience in hepatic interventions). A consistent approach according to our standard institutional protocol was used. Initially, all patients underwent multiple angiographic steps to define the hepatic arterial anatomy and to determine portal venous patency. For cTACE, patients were treated with selective (lobar or segmental) injections. A solution containing 100 mg of cisplatin, 50 mg of doxorubicin and 10 mg of mitomycin C in a 1:1 mixture with Lipiodol (Guerbet, France) was infused and followed by administration of 100- to 300- μ m-diameter microspheres (Embospheres, Merit Medical, USA). Substantial arterial flow reduction to the tumour was defined as the technical end point of the procedure. For radioembolization, all patients were subjected to angiographic evaluation and, if required, embolization of collateral arteries was performed. In order to evaluate the degree of hepato-pulmonary shunting and to detect gastrointestinal deposition, 5–6 mCi of ^{99m}Tc -labelled macroaggregated albumin was injected into the hepatic artery. This shunt study

preceded the treatment by at least 1 week. Depending on the extent of the disease within the liver, patients received either unilobar or bilobar (right and left) treatment in multiple sessions and no whole liver infusion was performed. The infusion of Y90 microspheres (TheraSpheres®, MDS Nordion, Ottawa, Canada) was performed in accordance with institutional radiation safety guidelines. All patients who received cTACE were admitted overnight. Patient who received Y90 radioembolization were discharged the same day of the procedure after clinical monitoring in the recovery area.

MR imaging technique

All patients included in this study underwent a standardized MRI protocol before and after the initial IAT. MRI was performed on a 1.5-Tesla scanner (Siemens Magnetom Avanto, Erlangen, Germany) using a phased array torso coil. The protocol included breath-hold unenhanced and contrast-enhanced (0.1 mmol/kg intravenous gadopentetate; Magnevist; Bayer, Wayne, NJ) T1-weighted three-dimensional fat-suppressed spoiled gradient-echo imaging (repetition time ms/ echo time ms, 5.77/2.77; field of view, 320–400 mm; matrix, 192 × 160; slice thickness, 2.5 mm; receiver bandwidth, 64 kHz; flip angle, 10°) in the hepatic arterial phase (20 s), portal venous phase (70 s) and delayed phase (3 min) [26, 27].

Imaging data evaluation

Tumour assessment was performed by two independent readers (a radiologist with 9 years of experience in abdominal MRI and a radiology resident). All measurements made by the two readers were done using standardized electronic calipers using Digital Imaging in Communications and Medicine (DICOM) files. Prior to the measurements, images were examined in axial, coronal and sagittal reconstructions in order to visually identify the largest tumour expansion (for diameter and enhancement, respectively). The respective slice with the largest expansion of the tumour was then used for individual manual measurements. Native T1 images as well as triphasic contrast-enhanced T1 images were used to visually distinguish tumour enhancement from false-positive hyperintense T1 signal (e.g. from haemorrhage) and measurements were performed on the portal venous phase images. The measurements were then averaged for the survival analysis. Any ambiguity regarding the selected plane (axial/coronal/sagittal) of measurement was resolved by consensus. A target lesion was defined as the largest, dominant lesion treated during the first session of IAT. A single targeted lesion per patient was selected for analysis. The analysis of multiple target lesions was omitted as previous studies did not confirm the benefit of this methodology [28, 29].

3D quantitative image analysis was performed by a radiologist (J.C.) with 1 year of experience with the software prototype used in the study (Medisys, Philips Research, Suresnes, France) [25]. The accuracy and reader-independent reproducibility of the semiautomatic tumour segmentation as well as the radiological–pathological correlation of the method were reported previously [22, 30–32]. The software employed a semiautomatic 3D tumour segmentation on the portal venous phase, ceMRI acquired before and after the initial session of IAT (Fig. 2a, b). The overall tumour volume was directly calculated on the basis of this segmentation (Fig. 2c, d). The qEASL calculation was based on image subtraction [25, 33]. In brief, the 3D segmentation mask was transferred onto the subtraction

image and a region of interest (ROI) was placed into extratumoral liver parenchyma as a reference in order to calculate the relative enhancement values within the tumour (Fig. 2e, f) [34]. The patient-specific, average signal intensity within the ROI was then defined as a threshold in order to estimate enhancement within the 3D mask. Subsequently, enhancing regions were expressed as a percentage of the previously calculated overall tumour volume and visualized using a colour map overlay on the portal venous phase MRI scan (Fig. 2e, f) [25]. Additional methodological specifications for tumour segmentation, the qEASL technique as well as the ROI specifications can be found in the supplementary material.

Additionally to the 3D quantitative techniques, the same target lesions were assessed using RECIST, World Health Organization (WHO), mRECIST and EASL guidelines [17, 18, 20, 35]. All measurements made by the two readers were averaged for the survival analysis. Figure 3 provides an overview of all anatomic and enhancement-based methods. Tumour response on follow-up MRI was quantified by calculating the changes in the measured parameters (lesion diameters for RECIST and mRECIST, sum of lesion diameters for WHO and EASL, absolute lesion volume for vRECIST and enhancing tumour volume for qEASL). On the basis of the degree of tumour response, patients were classified as responders (R) or non-responders (NR). As for the subgroups, patients with complete response (CR) and partial response (PR) were considered R, while patients with stable disease (SD) and progressive disease (PD) were considered NR. Table 1 illustrates the stratification criteria used in the present study for all techniques [21]. The cut-off values for both volumetric techniques (vRECIST and qEASL) were adjusted according to the thresholds used for the corresponding unidimensional parameters (RECIST and mRECIST) [20], while taking into account the equation for the calculation of spheroid volumes:

$$Volume = \frac{4}{3}\pi r^3$$

Accordingly, a reduction of the overall/enhancing lesion diameter by 30 % resulted in a concordant reduction of the volume by 65 %, which was then interpreted as tumour response (PR). By implication, an increase of the overall/enhancing lesion diameter by 20 % would be translated into a volumetric increase by 73 % and was interpreted as progressive disease (PD) [20].

Statistical analysis

All statistical computations were performed using the commercial statistical software GraphPad Prism (version 6, San Diego, California, USA) and SPSS (IBM, version 22.0, Armonk, NY, USA). The summary of data was performed using descriptive statistics. Count and frequency were used for categorical variables. Mean and range were used for continuous variables. The distribution of all radiologic measurements before and after IAT was evaluated using the Kolmogorov–Smirnov test. A non-Gaussian distribution was confirmed and a non-parametric Wilcoxon matched-pair test was used. The agreement of manual measurements between the radiological readers was assessed using a linear regression analysis in order to investigate the correlation of results. Pearson's correlation coefficient (R^2) was calculated and Bland–Altman plots were used for residual analysis. Cohen's kappa

coefficient was calculated for inter-reader agreement between both readers and used for non-3D criteria that provided a stratification between responders and non-responders. OS was defined from the date of the first IAT session until death, last available follow-up or the end-of-observation date (30 December 2013). Survival curves were estimated with the Kaplan–Meier method and plotted for each method, stratifying the patient collective into R and NR. The differences (R vs. NR) were assessed using the log-rank test. $P < 0.05$ was considered to indicate statistically significant differences. The median OS and the 95 % confidence interval (CI) for R and NR were calculated for every method. The predictive value of each radiological technique was assessed using Cox proportional hazard ratios (HR). This was followed by a univariate and multivariate analysis, which was performed in two steps. In the first step, a univariate Cox regression model was used to evaluate the association of overall survival with clinical factors assessed on baseline: gender, age, Eastern Cooperative Oncology Group (ECOG) performance score, status post (s/p) surgical resection of the primary tumour, s/p surgical resection of liver tumours, lines of chemotherapy, tumour burden as well as presence of extrahepatic disease. In the second step, adjusted hazard ratios for all radiological measurements were estimated from the Cox regression model which simultaneously included the respective radiological method as well as clinical factors that were found to be significantly predictive of overall patient survival ($P < 0.05$) [36].

Results

Patient characteristics

Table 2 summarizes the baseline characteristics of the selected patient cohort. Median patient age was 57.5 years (range, 43.8–88.2) and the majority of patients were male (79 %). All patients were classified as Child–Pugh A prior to the initial session of IAT. Median lesion size was 5.5 cm (mean, 6.8 cm; range, 1.4–17 cm). The majority of patients had multifocal liver disease (63 %) and almost half of the collective (47 %) were diagnosed with extrahepatic mCRC with lung and lymphatic nodes being the most common sites of the disease (57 % and 36 %, respectively).

Treatment, MRI acquisition and clinical outcome

Table 3 gives an overview of the treatment history and provides information on types of IAT as well as the frequency of the procedures. The majority of patients had undergone surgery of the primary tumour (86 %) as well as three or more lines of systemic chemotherapy (82 %), with a maximum of 10 cycles in one patient. All patients were considered to have unresectable and chemoresistant disease with IAT being the salvage option. All IAT sessions were technically successful and no major toxicity was reported. Four patients (14 %) underwent a crossover of IAT. In three cases, cTACE was chosen to follow an initial treatment with radioembolization while one remaining patient was treated in the reverse order. The mean interval between baseline imaging and IAT was 18.8 days (range, 1–38 days). The mean interval between IAT and the first follow-up MRI was 28 days (range, 19–43 days). Median OS of the entire population was 7.5 months (95 % CI, 5.2–10.1 months) (Fig. 4a). As for the univariate analysis of parameters used to characterize the patient cohort, ECOG performance status (ECOG 0, HR 3.9; 95 % CI, 1.9–15.4; $P < 0.001$) was identified

as the only parameter to be significantly correlated with overall survival ($P < 0.05$). When stratified according to treatment modality, no statistically significant differences in median OS were observed between the groups with 7.1 months (95 % CI, 4.2–11.5 months) and 9.3 months (95 % CI, 4.7–10.8 months) for the cTACE and radioembolization group, respectively ($P = 0.44$; HR, 1.1; 95 % CI, 0.5–2.7) (Fig. 4b).

MR imaging analysis

1D and 2D techniques—A total of 29 targeted lesions were assessed using the RECIST, WHO, mRECIST and EASL techniques. The changes in tumour parameters after IAT are illustrated in Fig. 5. The agreement between the two radiological readers was very good for RECIST ($R^2 = 0.93$) as well as for mRECIST ($R^2 = 0.88$) and good for EASL ($R^2 = 0.83$). WHO showed an adequate agreement between both readers ($R^2 = 0.77$). The results of the residual analysis are demonstrated using Bland–Altman plots in Fig. 1 in the supplementary material. When we used RECIST measurements, 25 patients (86 %) had SD and the remaining 4 patients (14 %) had PD. According to the WHO criteria, 26 patients (89 %) had SD and 3 patients (11 %) had PD. The use of both anatomic criteria did not classify any patients as responders after IAT; thus, no comparative survival analysis between R and NR was performed. When stratifying according to the enhancement-based EASL guideline, 13 patients (45 %) showed PR, 14 patients (48 %) had SD and 2 patients (7 %) had PD while no patient showed CR. According to mRECIST, a total of 8 patients (28 %) showed PR, 19 patients (66 %) had SD, 2 patients (7 %) had PD and none was identified as CR. The overall rate of R was higher for EASL as compared to mRECIST (45 % and 28 %, respectively). As for the reader-dependent classification of patients as responders vs. non-responders, Cohen's kappa coefficient was 0.852 (95 % CI 0.654–1.0) and 1.0 (95 % CI 1.0–1.0) for EASL and mRECIST, respectively.

When stratified according to the treatment modality using the EASL guideline, 5 patients (38 %) treated with cTACE had a PR, 8 patients (62 %) had SD and no patient showed PD. Within the radioembolization group, EASL identified 8 patients (50 %) as PR, 6 patients (37 %) as SD and 2 patients (13 %) had PD. According to mRECIST, 2 patients (15 %) treated with cTACE had PD and 11 patients (85 %) ($N = 11$) showed SD. For radioembolization, 6 patients (37 %) showed a PR and 8 patients (50 %) showed SD, while 2 patients (13 %) showed PD. Taken together, radioembolization showed a higher rate of R according to EASL and mRECIST (50 % and 37 %, respectively) as compared to cTACE (38 % and 15 % for EASL and mRECIST, respectively). However, both patients that showed PD (equally identified as such by EASL and mRECIST) were treated with radioembolization, while no patient treated with cTACE demonstrated PD. The association of tumour response according to the enhancement-based methods with OS did not result in a statistically significant stratification of R and NR (Fig. 4c, d; Table 4).

3D quantitative MRI analysis—A total of 29 patients were assessed using vRECIST and qEASL. As previously mentioned, Fig. 5 illustrates the changes in tumour parameters. When quantifying tumour response with vRECIST, 23 patients (79 %) had SD and 6 patients (21 %) showed PD. The use of vRECIST did not classify any patients as R. Thus, no comparative survival analysis between R and NR could be performed. When using the

qEASL technique, 10 patients (34 %) showed PR, 13 patients (45 %) had SD and 6 patients (21 %) PD, while no patient was classified as CR. The stratification of patients into R and NR after IAT was predictive of patient survival when using qEASL (Fig. 4e; Table 4), showing a significantly higher median OS in patients classified as R (HR 0.4; 95 % CI, 0.1–0.8; $P = 0.038$ for univariate analysis; $P = 0.024$ for multivariate analysis). Within this group, median OS was 9.9 months (95 % CI, 5.2–16.5 months) while NR achieved a median OS of 6.9 months (95 % CI, 3.3–8.8 months).

Using qEASL for the stratification of tumour response in patients treated with cTACE showed a PR in 4 patients (31 %), SD in 6 patients (46 %) and a PD in 3 patients (23 %) and no CR was achieved. For radioembolization, qEASL showed a PR in 6 patients (38 %), SD in 7 patients (44 %) and PD in 3 patients (18 %), while none achieved a CR. In summary, qEASL showed a slightly higher overall rate of R in patients treated with radioembolization (38 % vs. 31 % for cTACE).

Discussion

The main finding of this study identified qEASL as an early predictor of patient survival after IAT when assessing the dominant target lesion in patients with mCRC of the liver. In addition, all anatomic methods (RECIST, WHO, vRECIST) failed to stratify patients according to tumour response and did not predict patient survival. While achieving stratification between R and NR, the enhancement-based EASL and mRECIST failed to predict patient survival based on early follow-up MRI.

The ultimate goal of all imaging biomarkers of tumour response is the identification of NR after IAT [10]. In light of the overall dismal prognosis and a short life expectancy in the setting of salvage therapy, clinical decisions on whether or not to retreat a patient are frequently based on early imaging follow-up. A fundamental precondition for a successful stratification between R and NR is the diagnostic accuracy of the utilized technique. The most commonly used surrogate markers (EASL, mRECIST) have been primarily designed to simplify the assessment of hepatocellular carcinoma lesions before and after IAT [18, 20]. A direct translation of these techniques onto metastatic liver disease, specifically in patients with mCRC, proved inaccurate in our study and elsewhere [15, 19, 37, 38]. This can be mainly explained by the distribution of lesion enhancement and the nature of 1D and 2D measurements. These methods assume that 3D response to treatment occurs in a symmetrical, spherical manner. However, most liver tumours are prone to asymmetry and frequently demonstrate inhomogeneous patterns of necrosis induced by IAT [10, 15]. This is particularly the case in mCRC to the liver as most patients present after several lines of systemic chemotherapy. In these patients, baseline MRI typically demonstrates central necrosis as well as rim and segmental enhancement with scattered foci of remaining viable tumour tissue [39]. These characteristics underline the weaknesses of 1D and 2D techniques, providing the rationale for the use 3D quantitative approaches that are able to assess the entire extent of early tumour changes.

The 3D quantitative technique used in this study has several methodological strengths: First, this approach is based on a semiautomatic tumour segmentation, which enables a

reproducible, radio-pathologically validated and accurate volumetric lesion assessment [22, 30–32]. Furthermore, as opposed to fully automated segmentation techniques, a semiautomatic concept brings about the dual benefit of fast, software-based segmentation while allowing for a radiological reader to make adjustments, if necessary [22, 40]. Moreover, the image subtraction step allows for the quantification of true enhancement and facilitates an accurate quantification on the enhancing tissue on portal venous phase images. In addition, the use of an enhancement-based, 3D quantitative technique allows for this system to be translated onto other cross-sectional imaging modalities, such as cone-beam computed tomography (CBCT) as well as multi-detector CT (MDCT). This is particularly important in light of the advent of 3D quantitative intraprocedural tumour assessment on CBCT and may help overcome the limitations of inter-modality variability [41].

The patient population included in this analysis is representative of comparably designed studies regarding baseline characteristics (unresectable, liver-dominant or liver-only, chemorefractory disease) [8, 42–45]. As for the size of the cohort, the majority of published outcome studies for this subset of patients demonstrated similar or even smaller numbers of patients [46]. The necessary exclusion criteria further reduced the sample size because they were considered pivotal for a diagnostically accurate imaging analysis. These requirements outbalanced the desire for a slightly larger study population. In our study population, the median OS was 7.5 months, while no significant difference in OS between cTACE and radioembolization was observed. This result is in agreement with the available literature for this subset of patients, showing no modality-dependent differences of median OS and ranging from 6.9 to 10.5 months [7, 8, 42–45]. As for tumour response, no consistent data is available with criteria-dependent response rates ranging from 0 to 90 % [5, 37, 43, 47]. Interestingly, all enhancement-based criteria used in our study demonstrated slightly higher response rates for radioembolization, supporting the mounting evidence for the capability of this modality to achieve local tumour control [5, 45, 48]. However, this result must be confirmed with a prospective randomized trial in a significantly larger collective of patients. Overall, the inclusion of patients treated with both radioembolization and TACE into the analysis underlines the strength of the 3D quantitative technique to assess treatment response in a clinically realistic cohort and validates this analysis for both modalities. In our study, a volumetric quantification of tumour response required a definition of thresholds in order to correctly classify the patients. Accordingly, the parameters defined for mRECIST were translated onto vRECIST and qEASL [20]. However, this approach has been proven correct for hepatocellular carcinoma lesions only and lacks proper validation in metastatic liver disease. It must be therefore noted that additional studies that will use a split-sample cross-validation approach in larger cohorts are warranted in order to identify the ultimate cut-offs.

Our study has some limitations: First, the retrospective character of this analysis prevented us from enrolling a more homogenous patient population with regard to MRI protocol, treatment modality and history of the disease. However, this has been countered with reasonable exclusion criteria and a thorough multivariate analysis. The multivariate analysis was even more important in a non-therapy-naïve cohort in order to exclude potential bias through other treatment modalities when predicting survival based on image analysis. Second, our study protocol did not include the assessment of multiple target lesions.

However, several recent reports did not confirm the benefits of a multi-lesion assessment [28, 29]. Hence, it was decided to follow a clinically practicable approach in keeping the effect of radiological measurements as low as reasonably achievable. Third, the relatively short interval between IAT and tumour response assessment on MRI in patients treated with radioembolization can be seen as a double-edged sword with regard to the study design. There is evidence that tumours treated with radioembolization might exhibit the maximum of imaging response after 3 months. This happens because of the delayed and prolonged effects of radiation-based cytotoxicity and applies primarily to size-based criteria such as RECIST [49, 50]. However, tumour necrosis after radioembolization is frequently seen at earlier time points which can then result in a significant reduction of lesion enhancement, as measured in our study. Overall, measuring tumour response after 3 months did not concur with the goal of our study which aimed at providing a technique for an early assessment of treatment response in a patient cohort with a relatively short OS.

In summary, the ability of qEASL to predict overall patient survival early after IAT provides initial evidence for the potential advantage of 3D quantitative tumour analysis in mCRC patients treated with TACE or radioembolization. The enhanced diagnostic performance of qEASL, which leads to an improved stratification between R and NR, may very well help achieve consensus on the highly debated topic of tumour response assessment in this subset of patients.

Supplementary Material

Refer to Web version on PubMed Central for supplementary material.

Acknowledgements

The scientific guarantor of this publication is Jean-François Geschwind. The authors of this manuscript declare relationships with the following companies: JC, grant support: Rolf W. Günther Foundation for Radiological Sciences; RD, none; ML, Philips employee; RS, none; DL, Philips employee; ZW, none; LJS, grant support: Rolf W. Günther Foundation for Radiological Sciences; IRK, grant support: Siemens; JFG, consultant: Miocompatibles/BTG, Bayer HealthCare, Guerbet, Nordion/BTG, Philips HealthCare and Jennerex. Grant support: Biocompatibles/BTG, Bayer HealthCare, Philips Medical, Nodion/BTG, Threshold, Guerbet, DOD, NCI-ECOG and NIH-RO1. This study has received funding by NIH/NCI R01 CA160771, P30 CA006973, NCRR UL1 RR 025005, Philips Research North America, Briarcliff Manor, New York and the Rolf W. Günther Foundation for Radiological Sciences. Vivek Charu, Johns Hopkins Bloomberg School of Public Health kindly provided statistical advice for this manuscript.

Institutional review board approval was obtained. Written informed consent was waived by the institutional review board. Methodology: retrospective, diagnostic, prognostic study, performed at one institution.

References

1. Lozano R, Naghavi M, Foreman K, et al. Global and regional mortality from 235 causes of death for 20 age groups in 1990 and 2010: a systematic analysis for the Global Burden of Disease Study 2010. *Lancet*. 2012; 380:2095–2128. [PubMed: 23245604]
2. Engstrom PF, Arnoletti JP, Benson AB 3rd, et al. NCCN Clinical Practice Guidelines in Oncology: colon cancer. *J Natl Compr Canc Netw*. 2009; 7:778–831. [PubMed: 19755046]
3. Haddad AJ, Bani Hani M, Pawlik TM, Cunningham SC. Colorectal liver metastases. *Int J Surg Oncol*. 2011; 2011:285840. [PubMed: 22312501]
4. Cunningham D, Atkin W, Lenz HJ, et al. Colorectal cancer. *Lancet*. 2010; 375:1030–1047. [PubMed: 20304247]

5. Memon K, Lewandowski RJ, Riaz A, Salem R. Chemoembolization and radioembolization for metastatic disease to the liver: available data and future studies. *Curr Treat Options Oncol*. 2012; 13:403–415. [PubMed: 22773276]
6. Albert M, Kiefer MV, Sun W, et al. Chemoembolization of colorectal liver metastases with cisplatin, doxorubicin, mitomycin C, ethiodol, and polyvinyl alcohol. *Cancer*. 2011; 117:343–352. [PubMed: 20830766]
7. Benson AB 3rd, Geschwind JF, Mulcahy MF, et al. Radioembolisation for liver metastases: results from a prospective 151 patient multi-institutional phase II study. *Eur J Cancer*. 2013; 49:3122–3130. [PubMed: 23777743]
8. Hong K, McBride JD, Georgiades CS, et al. Salvage therapy for liver-dominant colorectal metastatic adenocarcinoma: comparison between transcatheter arterial chemoembolization versus yttrium-90 radioembolization. *J Vasc Interv Radiol*. 2009; 20:360–367. [PubMed: 19167245]
9. Kemeny NE, Niedzwiecki D, Hollis DR, et al. Hepatic arterial infusion versus systemic therapy for hepatic metastases from colorectal cancer: a randomized trial of efficacy, quality of life, and molecular markers (CALGB 9481). *J Clin Oncol*. 2006; 24:1395–1403. [PubMed: 16505413]
10. Gonzalez-Guindalini FD, Botelho MP, Harmath CB, et al. Assessment of liver tumor response to therapy: role of quantitative imaging. *Radiographics*. 2013; 33:1781–1800. [PubMed: 24108562]
11. Laubender RP, Lynghjem J, D'Anastasi M, et al. Evaluating the agreement between tumour volumetry and the estimated volumes of tumour lesions using an algorithm. *Eur Radiol*. 2014; 24:1521–1528. [PubMed: 24816938]
12. Huppert P, Wenzel T, Wietholtz H. Transcatheter arterial chemoembolization (TACE) of colorectal cancer liver metastases by irinotecan-eluting microspheres in a salvage patient population. *Cardiovasc Intervent Radiol*. 2014; 37:154–164. [PubMed: 23670568]
13. Narayanan G, Barbery K, Suthar R, Guerrero G, Arora G. Transarterial chemoembolization using DEBIRI for treatment of hepatic metastases from colorectal cancer. *Anticancer Res*. 2013; 33:2077–2083. [PubMed: 23645758]
14. Tohme S, Sukato D, Nace GW, et al. Survival and tolerability of liver radioembolization: a comparison of elderly and younger patients with metastatic colorectal cancer. *HPB (Oxford)*. 2014 doi:10.1111/hpb.12307.
15. Egger ME, Cannon RM, Metzger TL, et al. Assessment of chemotherapy response in colorectal liver metastases in patients undergoing hepatic resection and the correlation to pathologic residual viable tumor. *J Am Coll Surg*. 2013; 216:845–856. discussion 856–847. [PubMed: 23415549]
16. Akhlaghpour S, Aziz-Ahari A, Amoui M, Tolooee S, Poorbeigi H, Sheybani S. Short-term effectiveness of radiochemoembolization for selected hepatic metastases with a combination protocol. *World J Gastroenterol*. 2012; 18:5249–5259. [PubMed: 23066320]
17. Therasse P, Arbuck SG, Eisenhauer EA, et al. New guidelines to evaluate the response to treatment in solid tumors. European Organization for Research and Treatment of Cancer, National Cancer Institute of the United States, National Cancer Institute of Canada. *J Natl Cancer Inst*. 2000; 92:205–216. [PubMed: 10655437]
18. Bruix J, Sherman M, Llovet JM, et al. Clinical management of hepatocellular carcinoma. Conclusions of the Barcelona-2000 EASL conference. European Association for the Study of the Liver. *J Hepatol*. 2001; 35:421–430. [PubMed: 11592607]
19. Janne d'Othee B, Sofocleous CT, Hanna N, et al. Development of a research agenda for the management of metastatic colorectal cancer: proceedings from a multidisciplinary research consensus panel. *J Vasc Interv Radiol*. 2012; 23:153–163. [PubMed: 22264550]
20. Lencioni R, Llovet JM. Modified RECIST (mRECIST) assessment for hepatocellular carcinoma. *Semin Liver Dis*. 2010; 30:52–60. [PubMed: 20175033]
21. Riaz A, Memon K, Miller FH, et al. Role of the EASL, RECIST, and WHO response guidelines alone or in combination for hepatocellular carcinoma: radiologic-pathologic correlation. *J Hepatol*. 2011; 54:695–704. [PubMed: 21147504]
22. Bonekamp D, Bonekamp S, Halappa VG, et al. Interobserver agreement of semi-automated and manual measurements of functional MRI metrics of treatment response in hepatocellular carcinoma. *Eur J Radiol*. 2013 doi:10.1016/j.ejrad.2013.11.016.

23. Heijmen L, Ter Voert EE, Nagtegaal ID, et al. Diffusion-weighted MR imaging in liver metastases of colorectal cancer: reproducibility and biological validation. *Eur Radiol.* 2013; 23:748–756. [PubMed: 23001604]
24. Tam HH, Collins DJ, Brown G, et al. The role of pre-treatment diffusion-weighted MRI in predicting long-term outcome of colorectal liver metastasis. *Br J Radiol.* 2013; 86:20130281. [PubMed: 23995873]
25. Lin M, Pellerin O, Bhagat N, et al. Quantitative and volumetric European Association for the Study of the Liver and Response Evaluation Criteria in Solid Tumors measurements: feasibility of a semiautomated software method to assess tumor response after transcatheter arterial chemoembolization. *J Vasc Interv Radiol.* 2012; 23:1629–1637. [PubMed: 23177109]
26. Mitchell DG, Bruix J, Sherman M, Sirlin CB. LI-RADS (Liver Imaging Reporting and Data System): summary, discussion, consensus of the LI-RADS Management Working Group and future directions. *Hepatology.* 2014 10.1002/hep.27304.
27. Santillan CS, Tang A, Cruite I, Shah A, Sirlin CB. Understanding LI-RADS: a primer for practical use. *Magn Reson Imaging Clin N Am.* 2014; 22:337–352. [PubMed: 25086933]
28. Bogaerts J, Ford R, Sargent D, et al. Individual patient data analysis to assess modifications to the RECIST criteria. *Eur J Cancer.* 2009; 45:248–260. [PubMed: 19095437]
29. Kim BK, Kim SU, Kim MJ, et al. Number of target lesions for EASL and modified RECIST to predict survivals in hepatocellular carcinoma treated with chemoembolization. *Clin Cancer Res.* 2013; 19:1503–1511. [PubMed: 23225115]
30. Tacher V, Lin M, Chao M, et al. Semiautomatic volumetric tumor segmentation for hepatocellular carcinoma: comparison between C-arm cone beam computed tomography and MRI. *Acad Radiol.* 2013; 20:446–452. [PubMed: 23498985]
31. Chapiro J WL, Lin M, et al. A radiological-pathological analysis of contrast-enhanced and diffusion-weighted MRI in patients with HCC after TACE - testing the diagnostic accuracy of 3D quantitative image analysis. *Radiology.* 2014 in press.
32. Pellerin O, Lin M, Bhagat N, Ardon R, Mory B, Geschwind JF. Comparison of semi-automatic volumetric VX2 hepatic tumor segmentation from cone beam CT and multi-detector CT with histology in rabbit models. *Acad Radiol.* 2013; 20:115–121. [PubMed: 22947274]
33. Kim S, Mannelli L, Hajdu CH, et al. Hepatocellular carcinoma: assessment of response to transarterial chemoembolization with image subtraction. *J Magn Reson Imaging.* 2010; 31:348–355. [PubMed: 20099348]
34. Wagner M, Doblas S, Daire JL, et al. Diffusion-weighted MR imaging for the regional characterization of liver tumors. *Radiology.* 2012; 264:464–472. [PubMed: 22692032]
35. Miller AB, Hoogstraten B, Staquet M, Winkler A. Reporting results of cancer treatment. *Cancer.* 1981; 47:207–214. [PubMed: 7459811]
36. Bradburn MJ, Clark TG, Love SB, Altman DG. Survival analysis part III: multivariate data analysis - choosing a model and assessing its adequacy and fit. *Br J Cancer.* 2003; 89:605–611. [PubMed: 12915864]
37. Hips D, Ausania F, Manas DM, Rose JD, French JJ. Selective interarterial radiation therapy (SIRT) in colorectal liver metastases: how do we monitor response? *HPB Surg.* 2013; 2013:570808. [PubMed: 24285916]
38. Kekelidze M, D'Errico L, Pansini M, Tyndall A, Hohmann J. Colorectal cancer: current imaging methods and future perspectives for the diagnosis, staging and therapeutic response evaluation. *World J Gastroenterol.* 2013; 19:8502–8514. [PubMed: 24379567]
39. Koh DM, Brown G, Meer Z, Norman AR, Husband JE. Diagnostic accuracy of rim and segmental MRI enhancement of colorectal hepatic metastasis after administration of mangafodipir trisodium. *AJR Am J Roentgenol.* 2007; 188:W154–161. [PubMed: 17242222]
40. Gowdra Halappa V, Corona-Villalobos CP, Bonekamp S, et al. Neuroendocrine liver metastasis treated by using intraarterial therapy: volumetric functional imaging biomarkers of early tumor response and survival. *Radiology.* 2013; 266:502–513. [PubMed: 23192780]
41. Wang Z, Lin M, Lesage D, et al. Three-dimensional evaluation of Lipiodol retention in HCC after chemoembolization: a quantitative comparison between CBCT and MDCT. *Acad Radiol.* 2014; 21:393–399. [PubMed: 24507426]

42. Cosimelli M, Golfieri R, Cagol PP, et al. Multi-centre phase II clinical trial of yttrium-90 resin microspheres alone in unresectable, chemotherapy refractory colorectal liver metastases. *Br J Cancer*. 2010; 103:324–331. [PubMed: 20628388]
43. Huppert P, Wenzel T, Wietholtz H. Transcatheter arterial chemoembolization (TACE) of colorectal cancer liver metastases by irinotecan-eluting microspheres in a salvage patient population. *Cardiovasc Intervent Radiol*. 2013 doi:10.1007/s00270–013–0632-0.
44. Jakobs TF, Hoffmann RT, Dehm K, et al. Hepatic yttrium-90 radioembolization of chemotherapy-refractory colorectal cancer liver metastases. *J Vasc Interv Radiol*. 2008; 19:1187–1195. [PubMed: 18656012]
45. Sato KT, Omary RA, Takehana C, et al. The role of tumor vascularity in predicting survival after yttrium-90 radioembolization for liver metastases. *J Vasc Interv Radiol*. 2009; 20:1564–1569. [PubMed: 19846320]
46. Fiorentini G, Aliberti C, Mulazzani L, et al. Chemoembolization in colorectal liver metastases: the rebirth. *Anticancer Res*. 2014; 34:575–584. [PubMed: 24510986]
47. Mahnken AH, Pereira PL, de Baere T. Interventional oncologic approaches to liver metastases. *Radiology*. 2013; 266:407–430. [PubMed: 23362094]
48. Mulcahy MF, Lewandowski RJ, Ibrahim SM, et al. Radioembolization of colorectal hepatic metastases using yttrium-90 microspheres. *Cancer*. 2009; 115:1849–1858. [PubMed: 19267416]
49. Rosenbaum CE, Verkooijen HM, Lam MG, et al. Radioembolization for treatment of salvage patients with colorectal cancer liver metastases: a systematic review. *J Nucl Med*. 2013; 54:1890–1895. [PubMed: 24071510]
50. Camacho JC, Kokabi N, Xing M, Prajapati HJ, El-Rayes B, Kim HS. Modified response evaluation criteria in solid tumors and European Association for The Study of the Liver criteria using delayed-phase imaging at an early time point predict survival in patients with unresectable intrahepatic cholangiocarcinoma following yttrium-90 radioembolization. *J Vasc Interv Radiol*. 2014; 25:256–265. [PubMed: 24461131]

Key Points

- Volumetric assessment of colorectal liver metastases after intra-arterial therapy is feasible.
- Early 3D quantitative tumour analysis after intra-arterial therapy may predict patient survival.
- Volumetric tumour response assessment shows advantages over 1D and 2D techniques.
- Enhancement-based MR response assessment is preferable to size-based measurements.

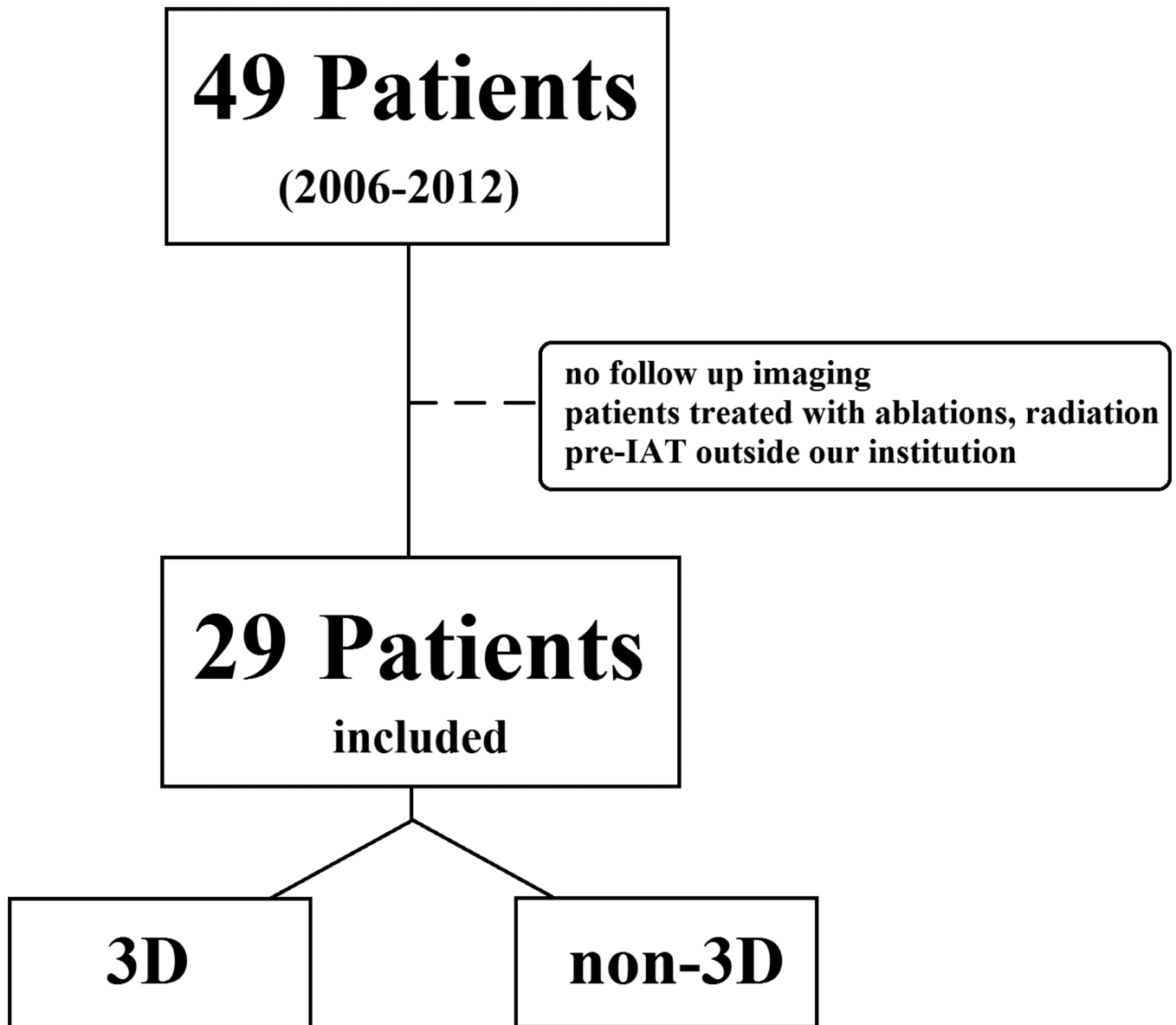


Fig. 1.
Flow chart illustrates the patient selection process as well as the most important exclusion criteria prior to imaging analysis

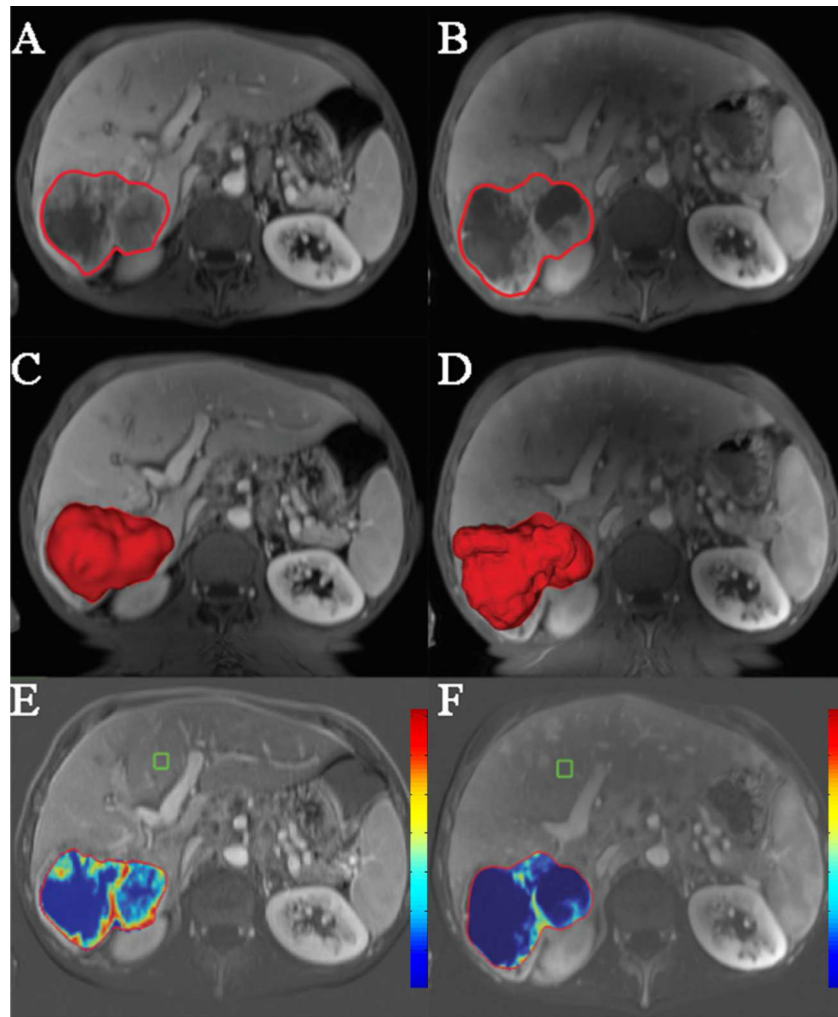


Fig. 2. 3D quantitative assessment technique. The *left column* represents baseline imaging, while the *right column* represents the follow-up MRI post TACE. **a, b** Semiautomated tumour segmentation on a representative, contrast-enhanced T1-weighted MR sequence. Of note, **a** and **b** are images prior to the subtraction. **c, d** Volume rendering for the segmented tumour in a 3D model of the upper abdomen. **e, f** qEASL colour maps of the tumour after subtraction (*red* maximum enhancement, *blue* no enhancement, normalized by the ROI). The selected patient had stable disease according to RECIST, WHO, vRECIST and partial response according to EASL, mRECIST and qEASL

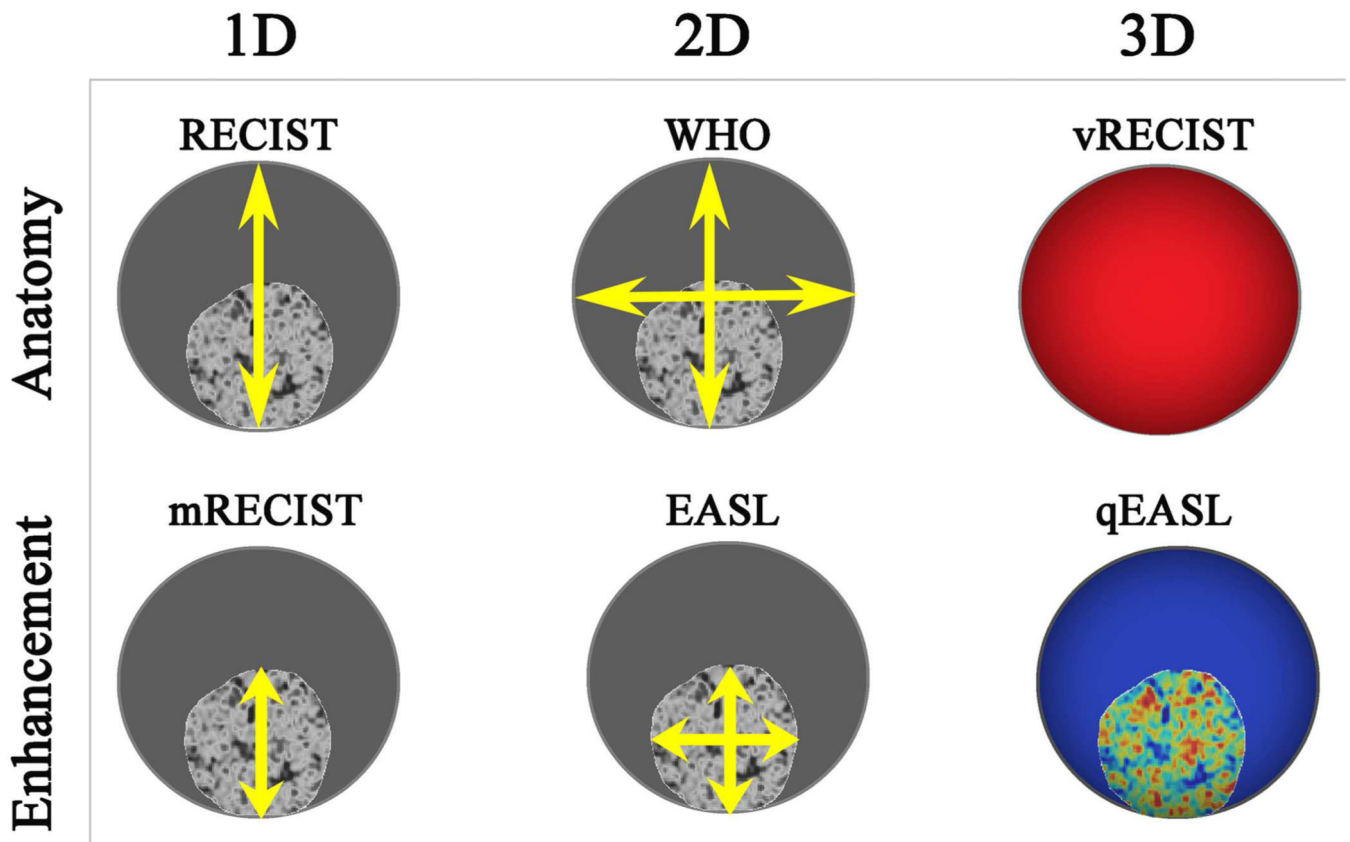


Fig. 3. Techniques of tumour response assessment. The methods can be divided into anatomic measurements (estimation of overall tumour diameter, area or volume) and enhancement-based measurements (estimation of viable tumour diameter, area or volume). According to the nature of the measurements, 1D techniques encompass unidirectional measurements of the tumour diameter (RECIST) or enhancing tissue diameter (mRECIST). 2D techniques measure the sum of overall tumor diameters (WHO) or the sum of the enhancing tumour diameters (EASL). 3D techniques measure the overall tumour volume (vRECIST), and enhancing tumour volume (qEASL)

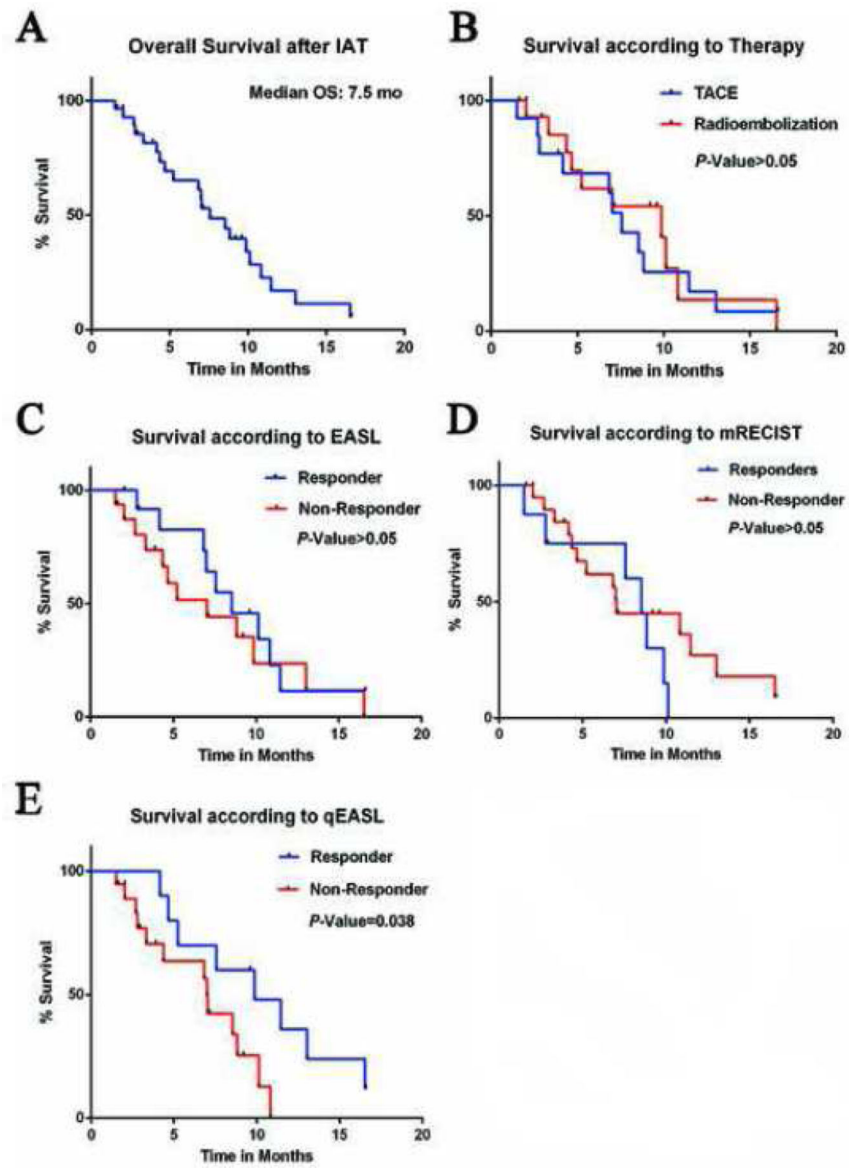


Fig. 4. Survival analysis for the entire patient population (a), stratified according to treatment modality (b) and based on the stratification according to tumour response (c–e)

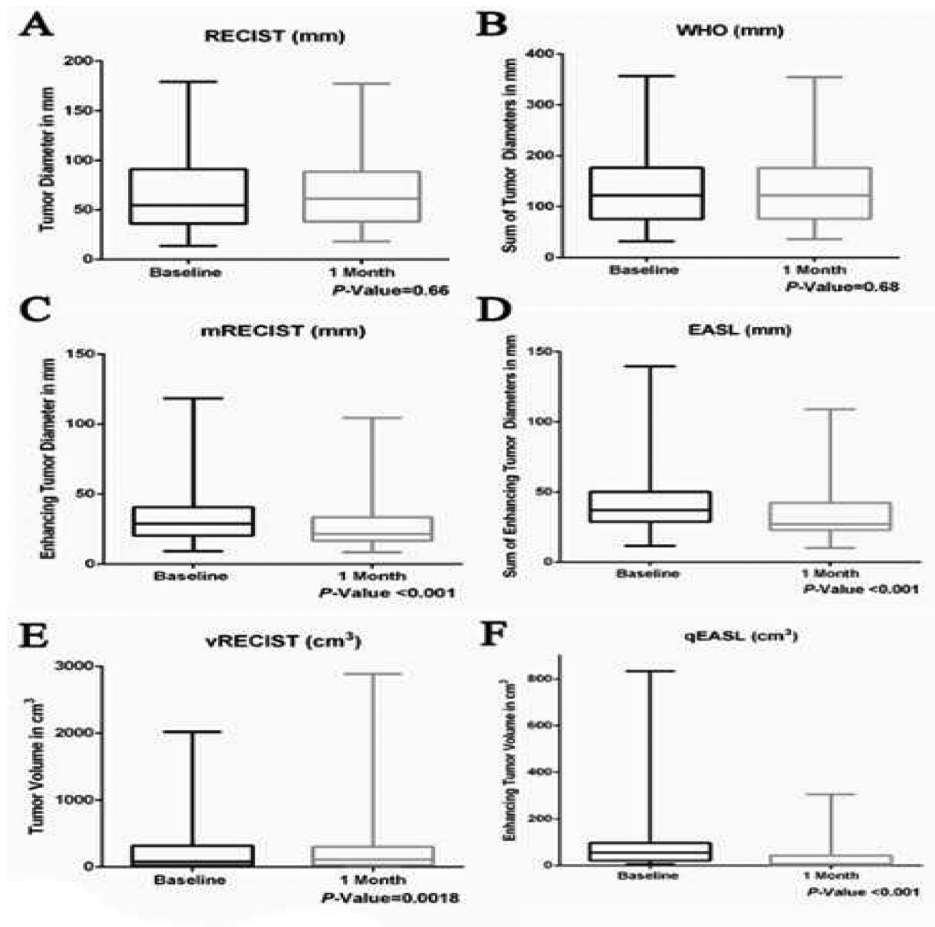


Fig. 5. Comparison of tumor characteristics before and after IAT. The figure demonstrates the measured parameters before and after treatment for all the applied tumor response assessment techniques. Enhancement-based techniques (mRECIST, EASL and qEASL) demonstrate statistically significant changes. No significant changes can be observed for anatomic techniques

Table 1

Definitions of tumour response

Evaluation method	Class	Subclasses of tumour response
RECIST	R	CR: complete disappearance of tumour
		PR: 30 % decrease
	NR	SD: criteria of PR/PD not met
		PD: 20 % increase
mRECIST	R	CR: complete disappearance of enhancement
		PR: 30 % decrease ^a
	NR	SD: criteria of PR/PD not met
		PD: 20 % increase ^a
WHO	R	CR: complete disappearance of tumour
		PR: 50 % decrease
	NR	SD: criteria of PR/PD not met
		PD: 20 % increase
EASL	R	CR: complete disappearance of enhancement
		PR: 50 % decrease ^b
	NR	SD: criteria of PR/PD not met
		PD: 20 % increase ^b
vRECIST	R	CR: complete disappearance of tumour
		PR: 65 % decrease
	NR	SD: criteria of PR/PD not met
		PD: 73 % increase
qEASL	R	CR: complete disappearance of enhancement
		PR: 65 % decrease ^c
	NR	SD: criteria of PR/PD not met
		PD: 73 % increase ^c

CR complete response, PR partial response, SD stable disease, PD progressive disease

^aIn the diameters of viable (enhancing) target lesion

^bIn the area of viable (enhancing) target lesion

^cIn the volume of viable (enhancing) target lesion

Table 2

Baseline patient characteristics

Parameter	N (%)	
Demographics		
Age, years	<65	21 (72)
	65	8 (28)
Sex	Male	23 (79)
	Female	6 (21)
ECOG performance status	0	20 (69)
	1	9 (31)
Bilirubin, mg/dL	Median	0.5
	Range	0.15–1.7
Albumin, g/dL	Median	3.9
	Range	3.1–5.3
Prothrombin time (INR)	Median	1.0
	Range	0.9–1.6
Tumour characteristics		
Tumour burden, %	<50	23 (79)
	50	6 (21)
Synchronous disease	Yes	11 (37)
	No	18 (63)
Extrahepatic metastases	Yes	14 (47)
	No	15 (53)
Tumour location	Bilobar	23 (79)
	Unilobar	6 (21)

ECOG Eastern Cooperative Oncology Group

Table 3

Treatment history

Parameter		N (%)
Previous systemic chemotherapy, lines	1–2	5 (18)
	>2	24 (82)
Previous surgery of the primary tumour	Yes	25 (86)
	No	4 (14)
Previous hepatic resection	Yes	4 (14)
	No	25 (86)
Interval from mCRC diagnosis to first IAT, months	Mean	18.8
	Median	15
	Range	1–57
Treatment modality	TACE	13 (45)
	Radioembolization	16 (55)
Frequency	Sessions, overall	54
	Mean/patient	1.9
	Range	1–4
	TACE	28 (52)
	Radioembolization	26 (48)
Patients with crossover of IAT	Yes	4 (14)
	No	25 (86)

mCRC metastatic colorectal cancer, *IAT* intra-arterial therapy, *TACE* transarterial chemoembolization

Table 4

Method	N (%)	Overall survival		Univariate analysis		Multivariate analysis	
		Median, months	95 % CI	HR (95 % CI)	P value	HR (95 % CI)	P value
RECIST							
R	0 (0)	-			-		-
NR	29 (100)	7.5	5.2-10.1	1.0		1.0	
mRECIST							
R	8 (28)	8.5	6.1-10.9	1.6 (0.6-4.9)	0.27	1.8 (0.8-5.2)	0.66
NR	21 (72)	7.0	6.6-7.4	1.0		1.0	
WHO							
R	0 (0)	-			-		-
NR	29 (100)	7.5	5.2-10.1	1.0		1.0	
EASL							
R	13 (45)	8.5	4.8-12.2	0.7 (0.3-1.7)	0.44	0.8 (0.4-1.9)	0.31
NR	16 (55)	7.0	2.8-11.2	1.0		1.0	
vRECIST							
R	0 (0)	-			-		-
NR	29 (100)	7.5	5.2-10.1	1.0		1.0	27
qEASL							
R	11 (37)	9.9	5.2-16.5	0.4 (0.1-0.8)	0.038	0.4 (0.1-0.8)	0.024
NR	18 (63)	6.9	3.3-8.8	1.0		1.0	